Electronic Supplementary Material (ESI) for Lab on a Chip.
This journal is © The Royal Society of Chemistry 2020

Supplementary Information

Acoustofluidic multi-well plates for enrichment of micro/nano particles and cells

Pengzhan Liu,[a,b] Zhenhua Tian,[c] Nanjing Hao,[a] Hunter Bachman,[a] Peiran Zhang,[a] Junhui Hu*[b] and Tony Jun Huang*[a]

a. Department of Mechanical Engineering and Materials Science, Duke University, Durham, NC 27708, USA.
b. State Key Lab of Mechanics and Control of Mechanical Structures, Nanjing University of Aeronautics and Astronautics, Nanjing 210016, China.
c. Department of Aerospace Engineering, Mississippi State University, Starkville, MS 39762, USA.

*Corresponding authors.

Emails: ejhhu@nuaa.edu.cn; tony.huang@duke.edu

Material properties of the piezoelectric ring

The piezoelectric ring is polarized in the thickness direction and has an electromechanical coupling coefficient K_{31} of 0.35, piezoelectric constants d_{33} and d_{31} of 450 × 10^{-12} m/V and -190 × 10^{-12} m/V, respectively, elastic constants Y_{33} and Y_{11} of 5.6 × 10^{10} N/m^2 and 7.6 × 10^{10} N/m^2, respectively, a mechanical quality factor Q_m of 100, a dissipation factor tanδ of 1.2%, and a density of 7800 kg/m^3.

Table S1. Material parameters used in the numerical simulations

Water	
Density	998.2 kg/m^3
Sound speed	1480 m/s
Dynamic viscosity	1.01×10^{-3} Pa·s
Bulk viscosity	2.82×10^{-3} Pa·s
Heat capacity at constant pressure	4190 J/(kg·K)
Isobaric thermal expansion coefficient	2.08×10^{-4} 1/K
Thermal conductivity	0.59 W/(m·K)
Isothermal compressibility	4.6×10^{-10} 1/Pa
Air	
Density	1.2 kg/m^3
Sound speed	343 m/s
Glass slide	
Density	2203 kg/m^3
Young's modulus	73.1 GPa
Poisson's ratio	0.17
Isotropic loss factor	0.01
Epoxy	
Density	1673 kg/m^3
Young's modulus	3.6 GPa
Poisson's ratio	0.36
Isotropic loss factor	0.1

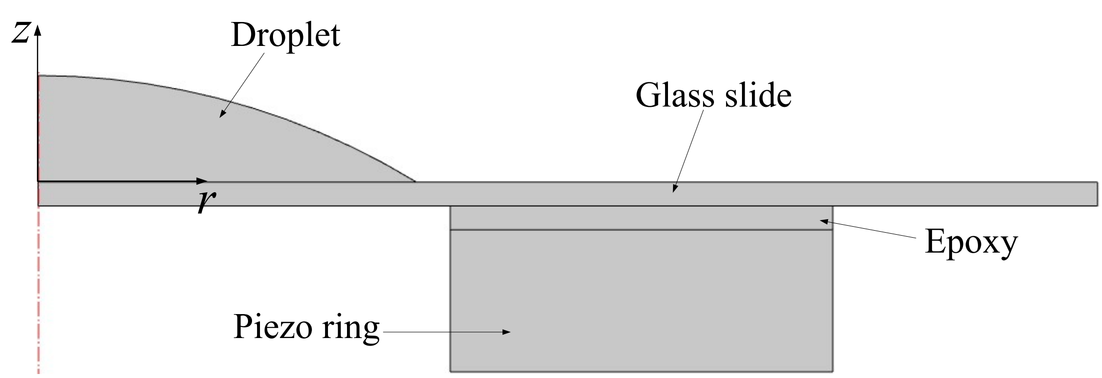

Figure S1. 2D axisymmetric physical model for numerical simulations.

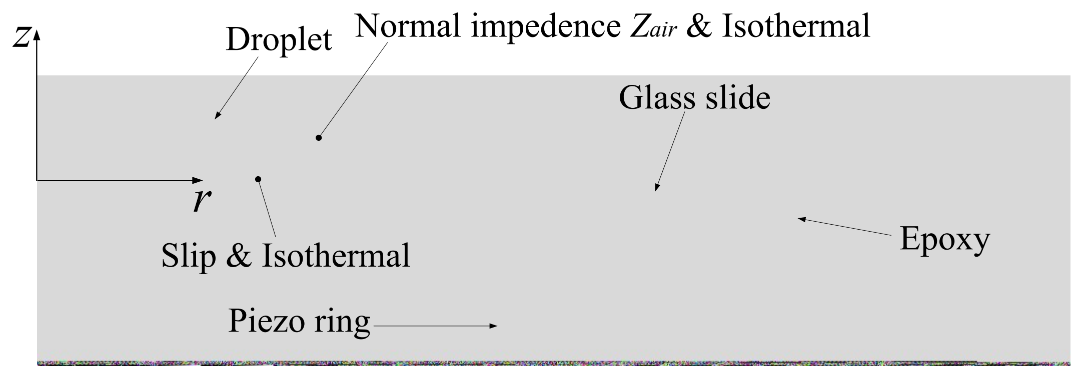

Figure S2. Boundary condition for simulation of acoustic field. (Z_{air} = 1.2 kg/m^3 × 343 m/s)

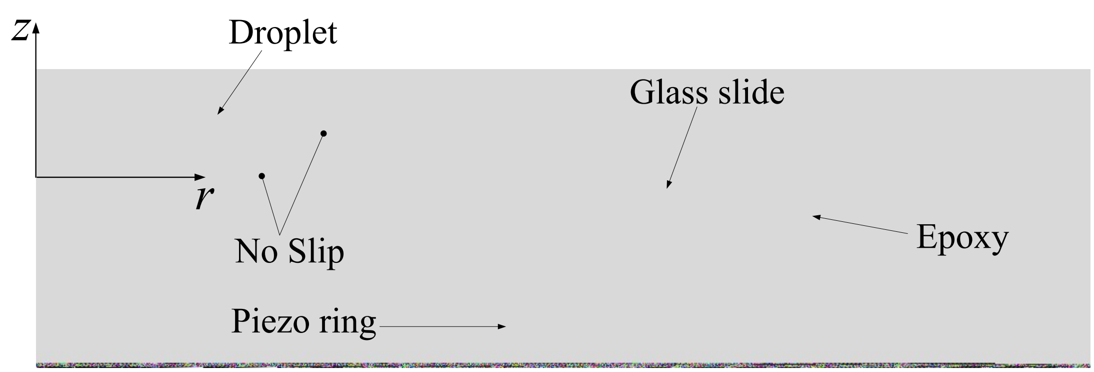

Figure S3. Boundary condition for simulation of acoustic streaming field.

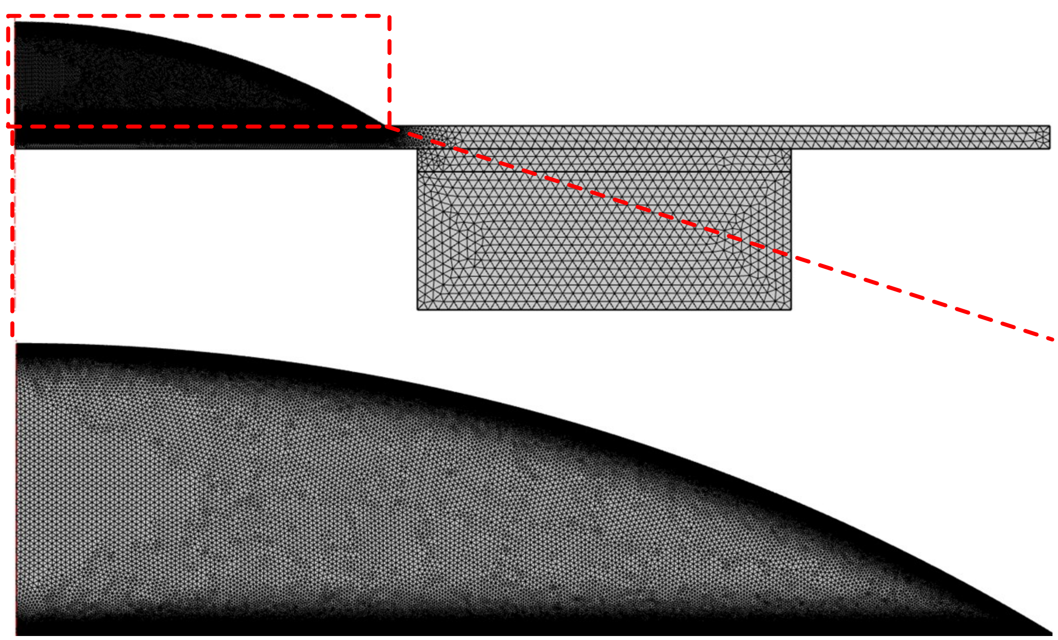

Figure S4. Mesh plot of the 2D axisymmetric model.

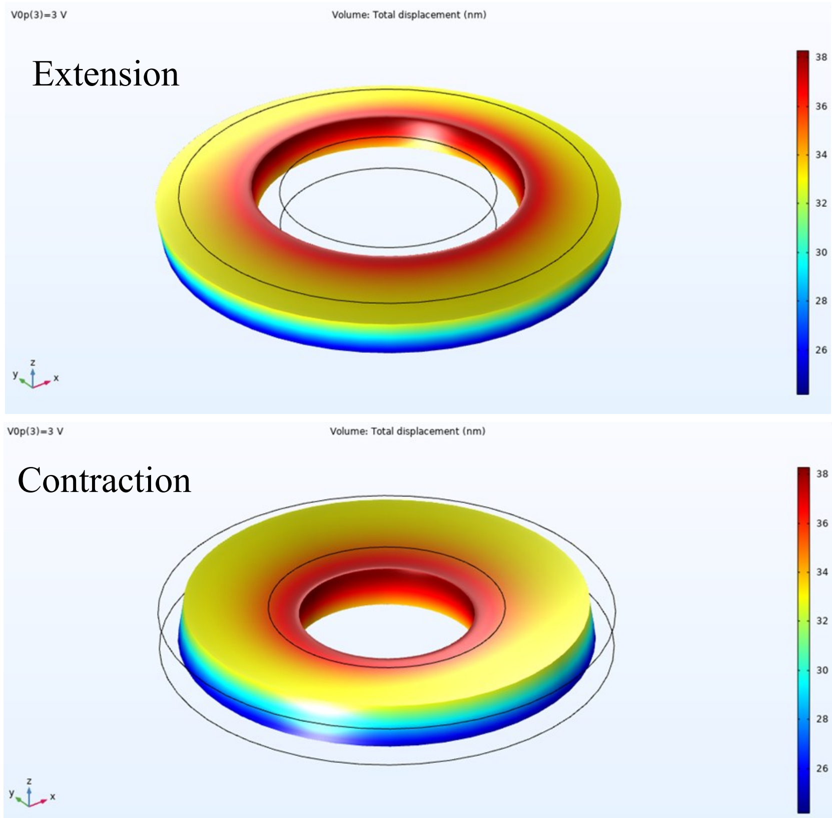

Figure S5. Radial extension vibration mode of the piezoelectric ring.

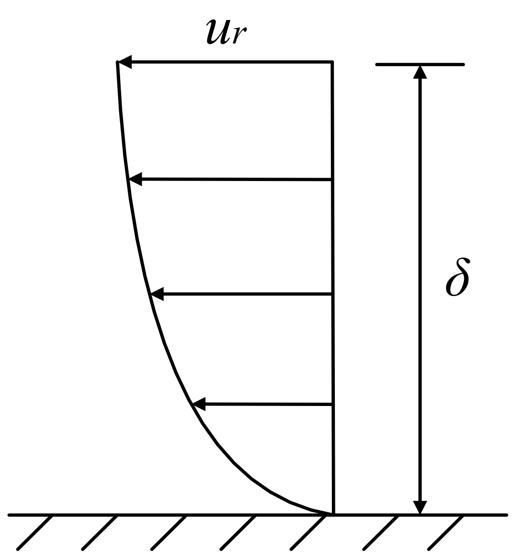

Figure S6. Acoustic streaming's profile in the viscous boundary layer.

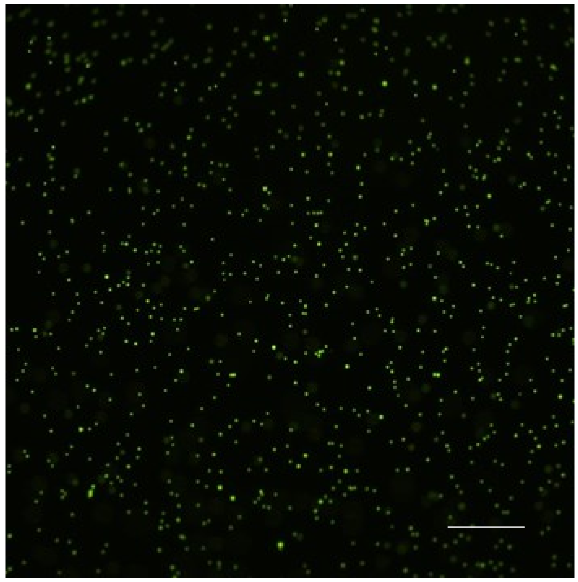

Figure S7. Initial distribution of 8 μm fluorescent polystyrene particles on the substrate in the panorama of the microscope. Scale bar: 500 μm.

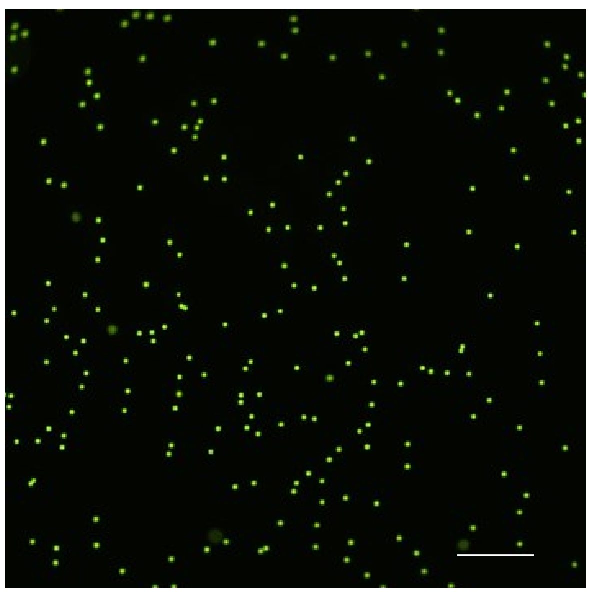

Figure S8. Initial distribution of 15 μm fluorescent polystyrene particles on the substrate in the panorama of the microscope. Scale bar: 500 μm.

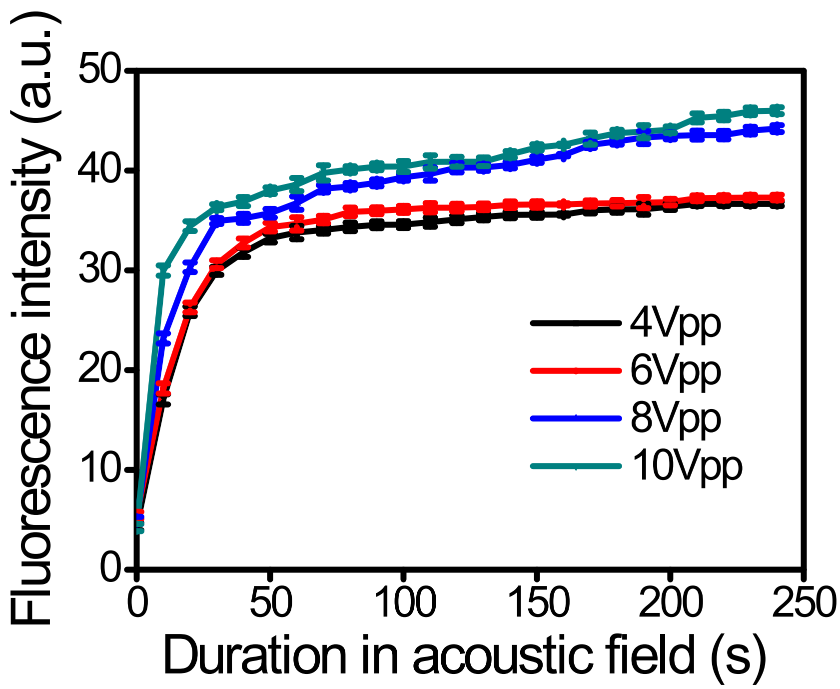

Figure S9. Fluorescence intensity versus acoustic field time under different driving voltages for 8 µm fluorescent polystyrene particles when the droplet volume and particle concentration are 15 µL and 0.10 mg/mL, respectively.

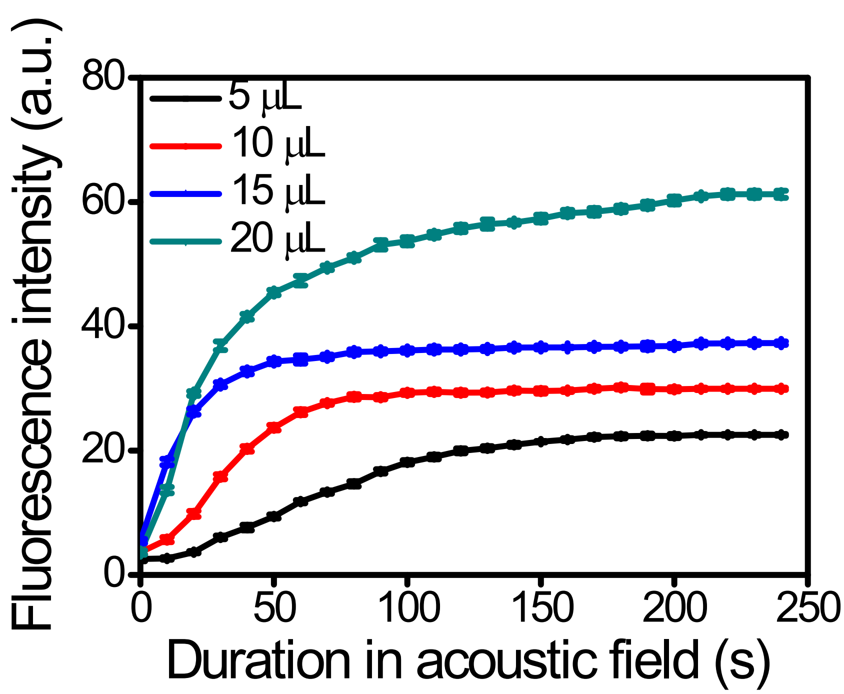

Figure S10. Fluorescence intensity versus acoustic field time under different droplet volumes for 8 µm fluorescent polystyrene particles when the driving voltage and particle concentration are 6 V_{pp} and 0.10 mg/mL, respectively.

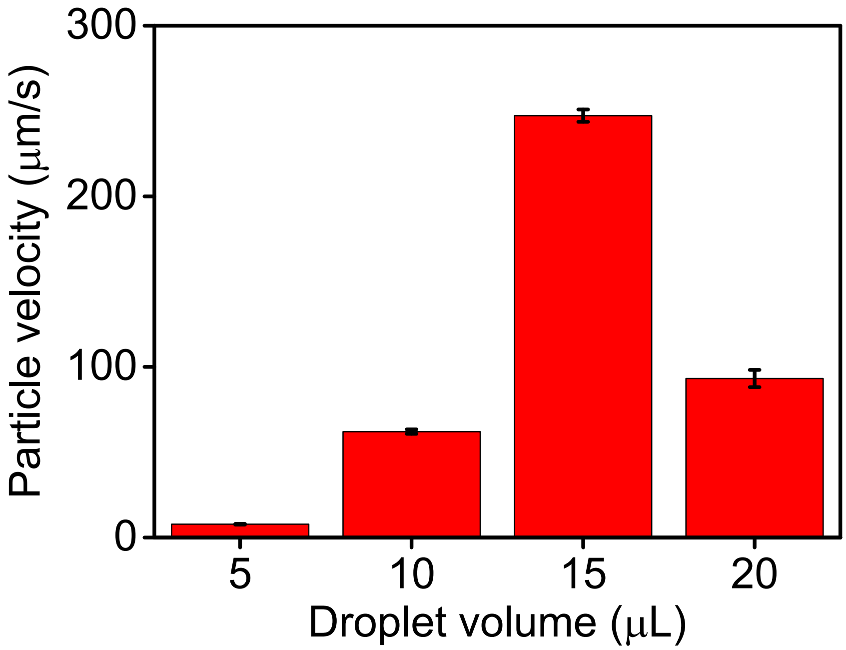

Figure S11. Measured mean motion velocity of single 15 μm fluorescent polystyrene particles versus droplet volume when the driving voltage and particle concentration were 6 V_{pp} and 0.20 mg/mL, respectively. Velocities taken as the average of 5 particles.

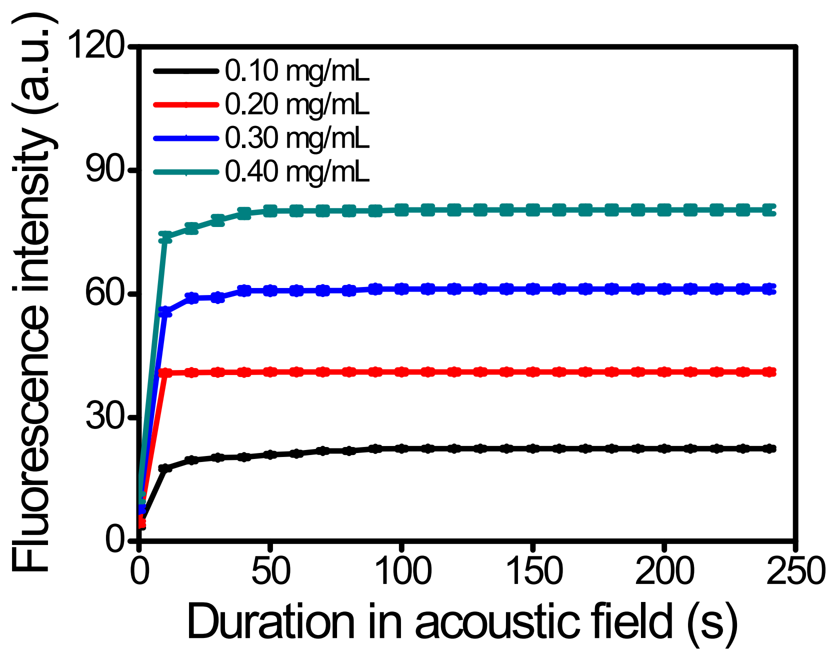

Figure S12. Fluorescence intensity versus acoustic field time under different particle concentrations for 15 μm fluorescent polystyrene particles when the driving voltage and droplet volume are 6 V_{pp} and 15 μL, respectively.

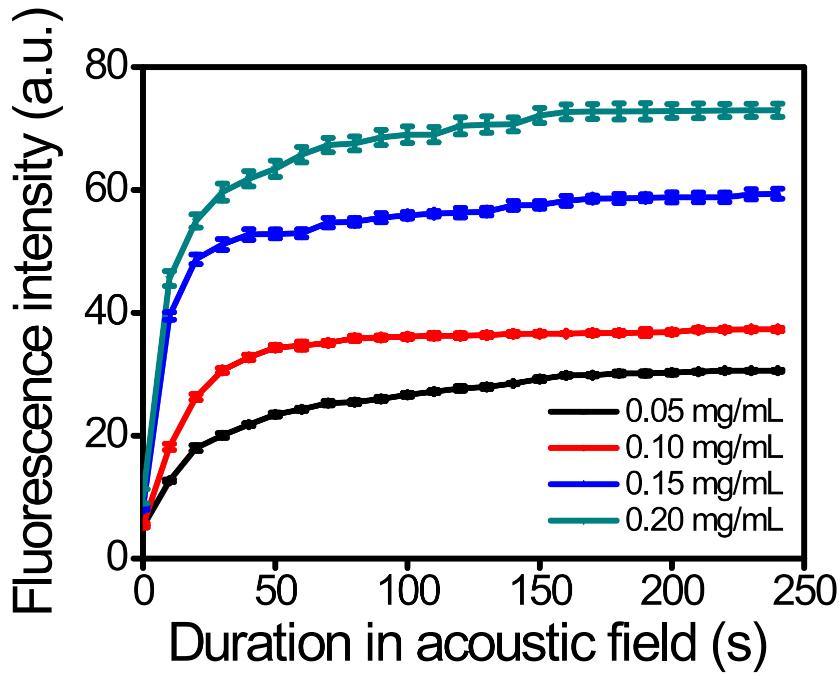

Figure S13. Fluorescence intensity versus acoustic field time under different particle concentrations for 8 μm fluorescent polystyrene particles when the driving voltage and droplet volume are 6 V_{pp} and 15 μL, respectively.

Force analysis of a single particle at the center of the droplet-substrate interface in the acoustofluidic field

Figure S14 shows a force schematic of a still single particle at the center of the droplet-substrate interface in the acoustofluidic field. The particle experiences a gravity force F_G, a buoyance F_B and a drag force induced by the vertical acoustic streaming F_D. Through numerical simulations, we found that the acoustic radiation force exerted on a single particle by the acoustic field can be negligible and is not considered here. The expressions of F_G, F_B and F_D are

$$F_G = \frac{4}{3}\pi R^3 \rho_P g \qquad (Eq1)$$

$$F_B = \frac{4}{3}\pi R^3 \rho_0 g \qquad (Eq2)$$

$$F_D = 6\pi\mu R v_{AS} \qquad (Eq3)$$

where R is the particle's radius, ρ_P is the particle's density, g is the gravity acceleration, ρ_0 is the water's density, μ is the water's shear viscosity and v_{AS} is the acoustic streaming velocity in the vertical direction. The condition that a single particle will not be lifted up by the upward acoustic streaming is that

$$\frac{F_G - F_B}{F_D} = \frac{2g}{9\mu v_{AS}} R^2(\rho_P - \rho_0) \geq 1 \qquad (F1)$$

It can be known from *F1* that larger and heavier particles are more susceptible to the enrichment accomplished by our device. When the particle's radius is in the range of the nanometer scale, it is difficult for polystyrene nanoparticles to satisfy *F1* since the density of polystyrene particles (1.05 g/cm^3) is very close to that of water. The density of the magnetic nanoparticles (1.7 g/cm^3) is much larger than water, so *F1* can be satisfied. The analysis indicates that with our device, it is easier to enrich microparticles than nanoparticles, and for nanoparticles, if the particle's density is too small, it may be very difficult to realize enrichment.

As an extension of this theoretical analysis, we consider a 200 nm-diameter nanoparticle as an example to determine the minimum density of particle that can be stably enriched. Figure S15 shows the distribution of the *z*-directional acoustic streaming velocity along the central axis of the droplet, which is extracted from Figure 2(d). From Figure S15, we can get the *z*-directional acoustic streaming velocity at h = 100 nm, which is the position of the mass center of a 200 nm-diameter nanoparticle, and the value is 0.0641 μm/s. With *F1*, we can deduce that for a 200 nm-diameter nanoparticle, theoretically, the minimum density that can be stably enriched is 3.9434 g/cm^3. Furthermore, it can be generally known from *F1* that when the particle size is determined, i.e., V_{AS} and R in *F1* are determined, the minimum density that can be stably enriched, i.e., ρ_P, can theoretically be determined.

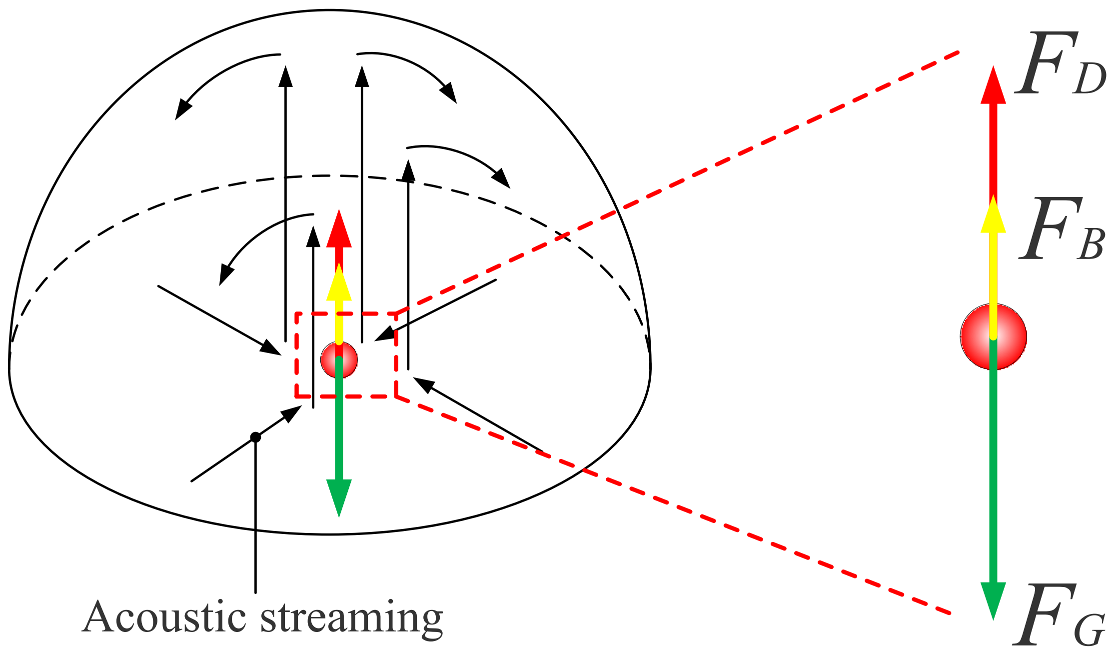

Figure S14. Force schematic of a still single particle at the center of the droplet-substrate interface in the acoustofluidic field.

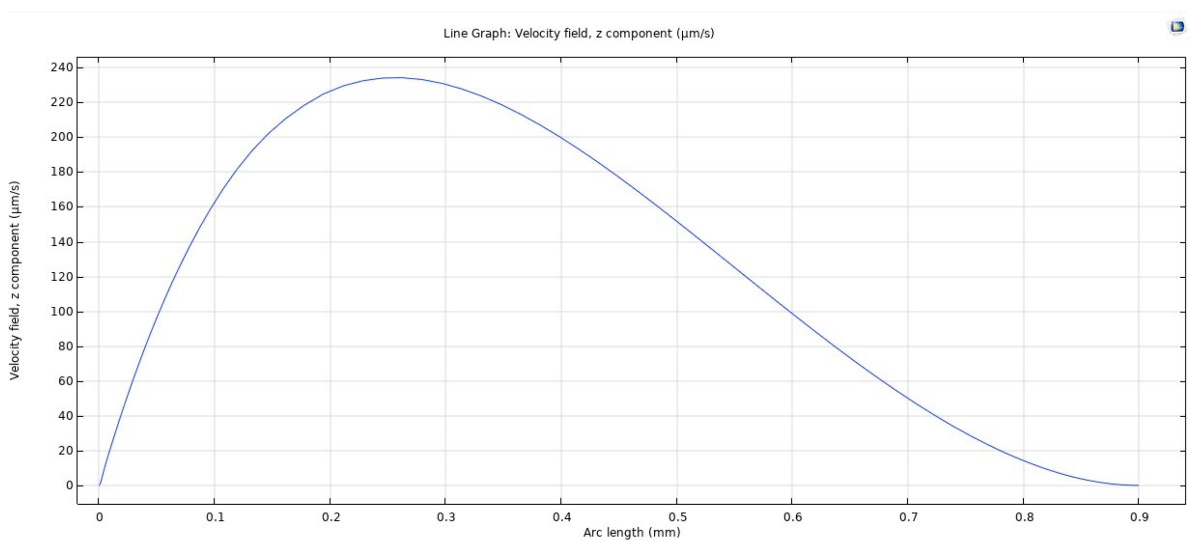

Figure S15. Distribution of the *z*-directional acoustic streaming velocity along the central axis of the droplet, which is extracted from Figure 2(d).

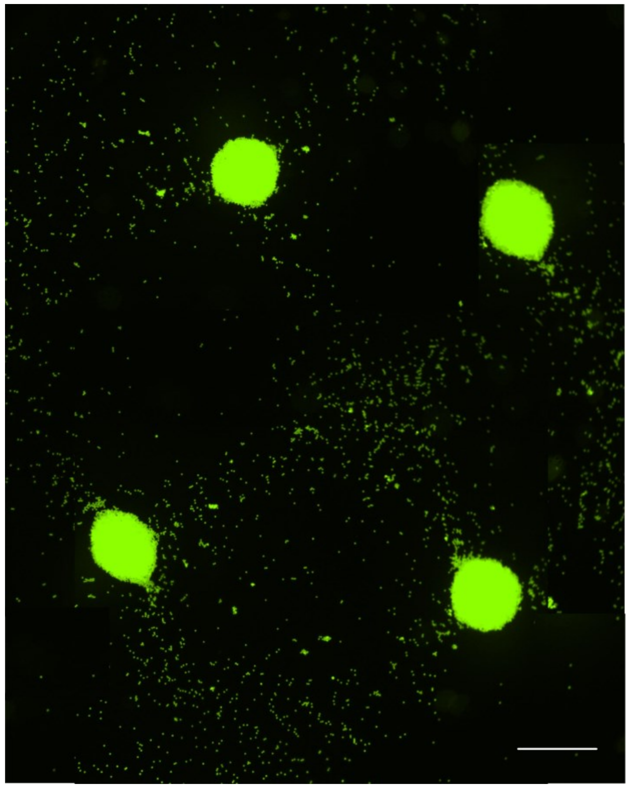

Figure S16. Four-spot enrichment of 10 µm fluorescent polystyrene particles realized by a single unit of the acoustofluidic multi-well plate with gel-based bonding when the driving voltage, frequency, and droplet volume are 10 V_{pp}, 97 kHz, and 20 µL, respectively. Scale bar: 500 µm. (Particle concentration: 0.20 mg/mL; duration in acoustic field: 2 min)

Movie S1. Enrichment of 8 µm fluorescent polystyrene particles.

Movie S2. Enrichment of 15 µm fluorescent polystyrene particles.